Human SIRT6 Promotes DNA End Resection Through CtIP Deacetylation

Abderrahmane Kaidi *et al.*

Science **329**, 1348 (2010);
DOI: 10.1126/science.1192049

Science (print ISSN 0036-8075; online ISSN 1095-9203) is published weekly, except the last week in December, by the American Association for the Advancement of Science, 1200 New York Avenue NW, Washington, DC 20005.

cells (fig. S14A). SR1 also abolished TCDD-induced, AHR-dependent transcription in cells expressing a human AhR–dependent luciferase reporter gene (hDRE-luc) (*15*), demonstrating that SR1 is a potent AHR antagonist [half-maximal inhibitory concentration (IC_{50}) = 127 nM] (fig. S14B). SR1 only weakly inhibited TCDD-induced transcription in murine cells and had no activity on rat cells, suggesting that SR1 preferentially inhibits human AHR. This observation correlates with the lack of activity of SR1 on murine HSCs and may explain the species selectivity of SR1 (table S9). We also tested two other AHR antagonists [alpha-naphthoflavone (*16*) and CH-223191 (*17*)], and both led to dose-dependent increases in the number of $CD34^+$ cells (fig. S15).

To elucidate whether the antagonizing effects of SR1 on AHR signaling are mediated by direct interaction with this nuclear receptor, we used a competitive binding assay between SR1 and AHR photoaffinity ligand (PAL) in liver cytosol isolated from h*AHR* transgenic mice (*18*). SR1 and the high-affinity AHR agonist (indirubin) both inhibited PAL binding (IC_{50} = 40 and 8 nM, respectively), whereas the inactive analog LGC006 was much less effective (IC_{50} = 9520 nM) (Fig. 4B and fig. S16). These results support the conclusion that SR1-induced $CD34^+$ cell expansion is mediated through direct binding and inhibition of the AHR.

To show a direct role for AHR in SR1-induced $CD34^+$ cell expansion, we infected CB $CD34^+$ cells with lentiviruses that express green fluorescent protein (GFP) and short hairpin–mediated RNAs (shRNAs) targeting AHR. In the $CD34^+GFP^+$ cells, both shRNAs led to decreases in AHR mRNA and protein expression (Fig. 4, C and D, and fig. S17A). shRNA knockdown of AHR led to sustained CD34 expression during culture, similar to that observed with SR1 (Fig. 4C and fig. S17, B and C). To determine if SR1-induced $CD34^+$ cell expansion requires inhibition of AHR activity, a constitutively active version of AHR lacking the ligand-binding domain (CA-AHR) was expressed (*19*). SR1 failed to inhibit hDRE-luc activity of HepG2 cells expressing CA-AHR, but it did inhibit dioxon-induced AhR activity in wild-type (WT) HepG2 cells and cells overexpressing WT AHR (fig. S18A). Similarly, SR1 had no effect on CB $CD34^+$ expressing CA-AHR (fig. S18B). Collectively, these data provide strong support that SR1 increases the number of CB-$CD34^+$ cells by direct binding and inhibition of the AHR.

Our data and that of others show that AHR is expressed in HSCs (*20*). In addition to its role as a ligand-activated transcription factor responsible for the induction of drug-metabolizing enzymes, AHR has been implicated in pathways regulating hematopoiesis, including HES-1–, c-MYC–, C/EBP-, PU.1-, β-catenin–, CXCR4-, and STAT5-dependent processes (*21*). Moreover, TCDD treatment of donor mice leads to a decrease in the reconstitution activity of $Lin^-cKit^+Sca\text{-}1^+$ cells (*22*, *23*). These findings strongly implicate AHR in HSC biology; however, future studies are required to define the molecular mechanisms involved in these processes.

One major question is whether the increase in SRC numbers elicited by SR1 reflects expansion of HSCs or indirect mechanisms, such as expansion of facilitator cells. The current data—which show that SR1 increases phenotypic HSC numbers, SR1 and AHR knockdown maintain CD34 expression, and SR1 expands multilineage CFUs—are consistent with AHR antagonists acting to promote SRC numbers by preventing differentiation of HSCs. However, the lack of a suitable in vivo transplantation assay capable of reading out the activity of single human HSCs makes it impossible to exclude alternative mechanisms. Better markers for human HSCs, bioassays capable of reading out single human HSCs, and clinical studies are required to address this important question.

Our results complement previously reported efforts to either enhance the expansion of HSCs [with Notch ligands, angiopoietins, copper chelators, glycogen synthase kinase 3β inhibitors, or the expression of *HOX* genes (*3*)] or increase HSC homing [with prostaglandin E2 (*24*), inhibition of CD26 (*10*), or fucosylation (*25*)] to improve HSC transplant outcomes. To this end, it will be important to explore the clinical potential of SR1, either by itself or in synergy with other agents, to improve outcomes and expand applications of autologous and allogeneic HSC transplantation.

References and Notes

1. M. Mimeault, R. Hauke, S. K. Batra, *Clin. Pharmacol. Ther.* **82**, 252 (2007).
2. M. Kondo *et al.*, *Annu. Rev. Immunol.* **21**, 759 (2003).
3. C. C. Hofmeister, J. Zhang, K. L. Knight, P. Le, P. J. Stiff, *Bone Marrow Transplant.* **39**, 11 (2007).
4. M. J. Mogul, *Bone Marrow Transplant.* **25** (suppl. 2), S58 (2000).
5. C. G. Brunstein, D. C. Setubal, J. E. Wagner, *Br. J. Haematol.* **137**, 20 (2007).
6. J. E. Wagner *et al.*, *Blood* **100**, 1611 (2002).
7. A. R. Smith, J. E. Wagner, *Br. J. Haematol.* **147**, 246 (2009).
8. L. J. Murray *et al.*, *Exp. Hematol.* **27**, 1019 (1999).
9. M. Z. Ratajczak, *Curr. Opin. Hematol.* **15**, 293 (2008).
10. T. B. Campbell, G. Hangoc, Y. Liu, K. Pollok, H. E. Broxmeyer, *Stem Cells Dev.* **16**, 347 (2007).
11. Materials and methods are available as supporting material on *Science* Online.
12. S. Ding, N. S. Gray, X. Wu, Q. Ding, P. G. Schultz, *J. Am. Chem. Soc.* **124**, 1594 (2002).
13. M. Ito *et al.*, *Blood* **100**, 3175 (2002).
14. S. S. Kelly, C. B. Sola, M. de Lima, E. Shpall, *Bone Marrow Transplant.* **44**, 673 (2009).
15. P. M. Garrison *et al.*, *Fundam. Appl. Toxicol.* **30**, 194 (1996).
16. J. Y. Jang *et al.*, *Reprod. Toxicol.* **24**, 303 (2007).
17. S. H. Kim *et al.*, *Mol. Pharmacol.* **69**, 1871 (2006).
18. C. A. Flaveny, I. A. Murray, C. R. Chiaro, G. H. Perdew, *Mol. Pharmacol.* **75**, 1412 (2009).
19. J. McGuire, K. Okamoto, M. L. Whitelaw, H. Tanaka, L. Poellinger, *J. Biol. Chem.* **276**, 41841 (2001).
20. M. Frericks, M. Meissner, C. Esser, *Toxicol. Appl. Pharmacol.* **220**, 320 (2007).
21. K. P. Singh, F. L. Casado, L. A. Opanashuk, T. A. Gasiewicz, *Biochem. Pharmacol.* **77**, 577 (2009).
22. K. P. Singh, A. Wyman, F. L. Casado, R. W. Garrett, T. A. Gasiewicz, *Carcinogenesis* **30**, 11 (2008).
23. R. Sakai *et al.*, *Toxicol. Sci.* **72**, 84 (2003).
24. T. E. North *et al.*, *Nature* **447**, 1007 (2007).
25. L. Xia, J. M. McDaniel, T. Yago, A. Doeden, R. P. McEver, *Blood* **104**, 3091 (2004).

26. We thank C. Trussell, D. Rines, and M. Hull for assistance with flow cytometry and screen development; J. E. Tellew, S. Pan, Y. Wan, and X. Wang for synthesis of LGC006; and J. Hogenesch for helpful discussions. A.E.B was funded by grants from the California Institute for Regenerative Medicine and the Skaggs Institute for Chemical Biology. M.S.D. was funded by grants from the National Institutes of Environmental Health Sciences (ES007685 and ES04699). G.H.P. was funded by a grant from the NIH (ES004869). A patent application has been filed on SR1 for applications related to HSC expansion.

Supporting Online Material

www.sciencemag.org/cgi/content/full/science.1191536/DC1
Materials and Methods
Figs. S1 to S18
Tables S1 to S9

27 April 2010; accepted 7 July 2010
Published online 5 August 2010;
10.1126/science.1191536
Include this information when citing this paper.

Human SIRT6 Promotes DNA End Resection Through CtIP Deacetylation

Abderrahmane Kaidi,[1] Brian T. Weinert,[2] Chunaram Choudhary,[2] Stephen P. Jackson[1]*

SIRT6 belongs to the sirtuin family of protein lysine deacetylases, which regulate aging and genome stability. We found that human SIRT6 has a role in promoting DNA end resection, a crucial step in DNA double-strand break (DSB) repair by homologous recombination. SIRT6 depletion impaired the accumulation of replication protein A and single-stranded DNA at DNA damage sites, reduced rates of homologous recombination, and sensitized cells to DSB-inducing agents. We identified the DSB resection protein CtIP [C-terminal binding protein (CtBP) interacting protein] as a SIRT6 interaction partner and showed that SIRT6-dependent CtIP deacetylation promotes resection. A nonacetylatable CtIP mutant alleviated the effect of SIRT6 depletion on resection, thus identifying CtIP as a key substrate by which SIRT6 facilitates DSB processing and homologous recombination. These findings further clarify how SIRT6 promotes genome stability.

Double-strand breaks (DSBs) are highly cytotoxic DNA lesions that can be repaired by homologous recombination, a highly coordinated process restricted to the S and G_2 phases of the cell cycle (*1*, *2*). Homologous recombination is instigated by DSB end resection (*3*, *4*), which generates single-stranded DNA (ssDNA) through the combined actions of proteins that

include CtIP [C-terminal binding protein (CtBP) interacting protein] (*5*, *6*) and the tumor suppressor protein BRCA1 (*7*). This ssDNA is bound by replication protein A (RPA), leading to the formation of a ssDNA-RAD51 nucleoprotein filament that mediates homologous recombination. Regulation of these events is critical for cell survival under both normal and DNA-damaging conditions; inherited or acquired deficiencies in DNA repair cause developmental defects, infertility, immune deficiency, neurodegenerative disease, heightened cancer predisposition, and aspects of premature aging (*8*).

We examined the effects of two protein lysine deacetylase (KDAC) inhibitors (*9*, *10*) on DNA damage response signaling triggered by camptothecin (CPT), a topoisomerase I inhibitor that induces replication-dependent DSBs that are repaired by homologous recombination. Sodium butyrate (NaB) inhibits class I and class II KDACs (*10*), whereas nicotinamide inhibits the NAD^+ (nicotinamide adenine dinucleotide)–dependent sirtuin (class III) family of KDACs (SIRT1 to SIRT7) (*9*). We initially confirmed the efficacy of KDAC inhibitors in human U2OS cells (fig. S1, A and B) and found that such treatments did not appreciably affect cell cycle profiles (fig. S1C). Although NaB did not affect CPT-induced DNA damage response signaling (Fig. 1A), nicotinamide specifically impaired RPA phosphorylation on Ser^4 and Ser^8 (Fig. 1A), a marker for resected CPT-induced DSBs (*5*, *11*). Consistent with this finding, nicotinamide-treated cells were impaired in forming RPA and ssDNA foci at CPT-induced lesions (Fig. 1B). Similar defects in RPA phosphorylation and formation of RPA foci were observed in human HeLa cells pretreated with nicotinamide (fig. S2, A and B). Nicotinamide not only impaired resection but also inhibited the CPT-induced formation of RAD51 foci (fig. S3, A and B), decreased homologous recombination (Fig. 1C) (*12*), and caused CPT hypersensitivity (Fig. 1D). Similarly, nicotinamide impaired resection-dependent signaling after treatment of cells with the topoisomerase II inhibitor etoposide (Fig. 1E). The failure of nicotinamide to inhibit phosphorylation of the checkpoint kinase CHK2 or the histone H2AX is consistent with these marks being independent of resection. However, upon nicotinamide treatment we noted essentially normal CHK1 phosphorylation (a mark associated with resected CPT-induced DSBs; fig. S3C), which suggests that CHK1 activation has a low threshold for resection.

Thus, DSB resection and homologous recombination are likely promoted by a KDAC of the sirtuin family. Of the seven human sirtuins, only SIRT1, SIRT6, and SIRT7 are nuclear (*13*), with SIRT1 (*14*, *15*) and SIRT6 (*16*–*18*) having been implicated in maintaining genome integrity. We found that small interfering RNA (siRNA)–mediated SIRT1 depletion caused no discernible defects in DNA damage response signaling (Fig. 2A). In contrast, although SIRT6 depletion did

[1]Gurdon Institute and Department of Biochemistry, University of Cambridge, Tennis Court Road, Cambridge CB2 1QN, UK. [2]NNF Center for Protein Research, Faculty of Health Sciences, University of Copenhagen, Blegdamsvej 3B, DK-2200 Copenhagen, Denmark.

*To whom correspondence should be addressed. E-mail: s.jackson@gurdon.cam.ac.uk

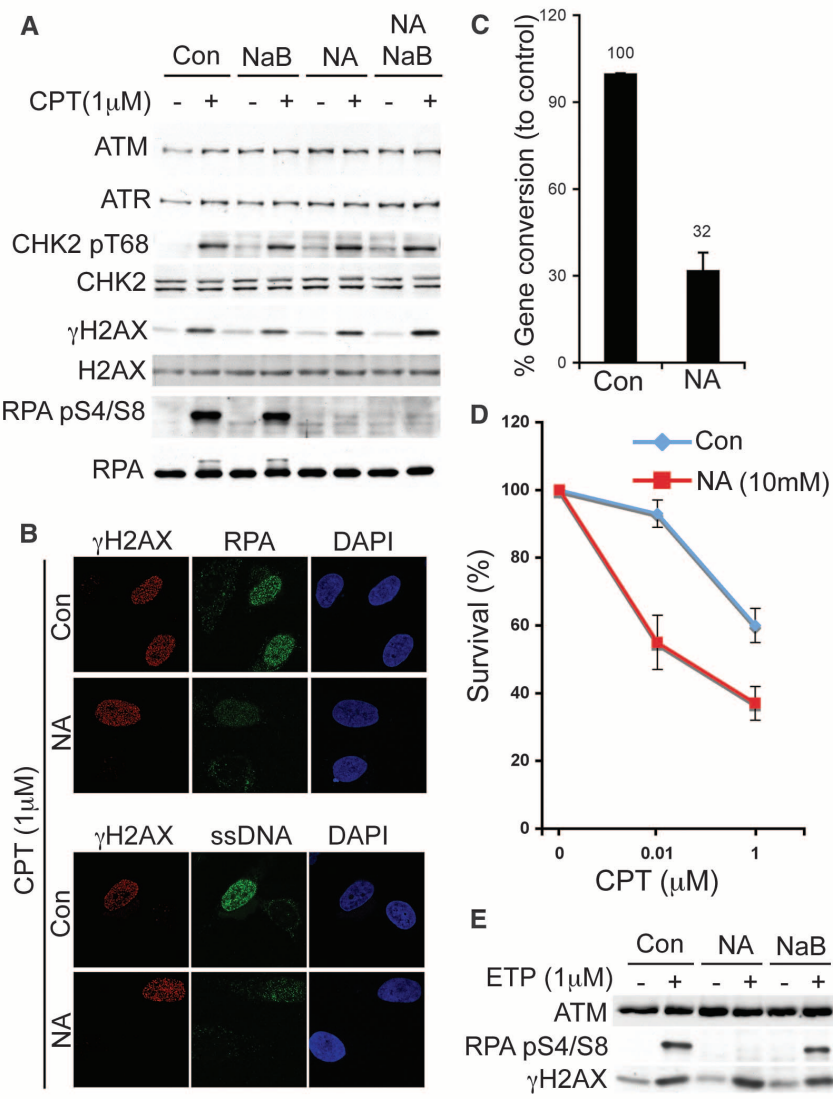

Fig. 1. Nicotinamide treatment impairs resection and homologous recombination. (**A**) U2OS cells were untreated (Con) or pretreated with nicotinamide (NA) and/or NaB, then exposed to CPT. Cell extracts were analyzed by Western blotting. ATM, ATR, CHK2, and H2AX are described in the text; CHK2 pT68, CHK2 phosphorylated on Thr^{68}; γH2AX, phosphorylated histone H2AX Ser^{139}; RPA pS4/S8, RPA phosphorylated on Ser^4 and Ser^8. (**B**) U2OS cells were treated and examined by immunofluorescence. ssDNA was detected with antibody to 5-bromo-2′-deoxyuridine. DAPI, 4′,6-diamidino-2-phenylindole. (**C**) Homologous recombination (gene conversion) was measured [(*12*); see also supporting online material]. Data from three experiments are presented as means ± SD. (**D**) U2OS survival upon CPT treatment in the presence or absence of nicotinamide. Results represent three experiments; error bars denote SD. (**E**) U2OS cells were treated as in (A) with 1 μM etoposide (ETP).

not affect phosphorylation of CHK2 or H2AX after CPT treatment, it markedly diminished CPT-induced RPA phosphorylation and the formation of RPA and ssDNA foci, thereby mirroring the effects of nicotinamide (Fig. 2, A to C). We detected similar resection impairments with various SIRT6 siRNAs (SIRT6-1-3; fig. S4, A and B) and in different human cell types (fig. S4C). Furthermore, *Sirt6*$^{-/-}$ mouse embryonic stem cells (ESCs) were impaired in CPT-induced RPA phosphorylation (Fig. 2D). Accordingly, SIRT6 depletion reduced homologous recombination frequencies (Fig. 2E) and sensitized cells to CPT (Fig. 2F). SIRT6 depletion also rendered cells hypersensitive to inhibition of poly(ADP-ribose) polymerase (PARP; Fig. 2G), which is selectively cytotoxic to homologous recombination–deficient cells (*19*, *20*). Despite exhibiting a proficient G_2-M DNA damage checkpoint (fig. S5, A and B) presumably due to efficient CHK1 phosphorylation (fig. S5C), SIRT6-depleted cells were also hypersensitive to ionizing radiation (fig. S5D) (*18*, *21*). SIRT6 depletion had no discernible effects on cell cycle profiles (figs. S5A and S6A) or cell proliferation (fig. S6, A and B), nor did it cause pronounced apoptotic cell death (fig. S6C).

To determine how SIRT6 regulates resection, we generated stable cell lines expressing siRNA-resistant, green fluorescent protein (GFP)–tagged wild-type SIRT6 or an enzymatically inactive SIRT6 [His^{133} → Tyr (H133Y); fig. S7]. After depleting endogenous SIRT6, cells expressing wild-type but not mutant SIRT6 were proficient in CPT-induced RPA phosphorylation and formation of RPA foci (Fig. 3, A and B, and fig. S8). Thus, SIRT6 catalytic activity promotes resection-associated events. We found that SIRT6 depletion or nicotinamide treatment had no obvious effects on the levels of known DSB resection proteins and did not affect the recruitment of such proteins to DNA damage sites (fig. S9). Consistent with SIRT6 controlling resection more directly while displaying a chromatin association profile that did not alter detectably in response to CPT treatment (Fig. 3C), GFP-SIRT6 accumulated rapidly at sites of laser-induced DNA damage (Fig. 3D). These results suggested that SIRT6 might directly associate with DSB resection factors. Accordingly, when we purified GFP-SIRT6 from human cells (Fig. 3E), mass spectrometry identified the DSB resection protein CtIP. This interaction was confirmed by coimmunoprecipitation analyses [Fig. 3F; SIRT6 immunoprecipitates also contained BRCA1, a known CtIP interactor (*22*)] and appears to be direct, as indicated by assays with purified proteins (fig. S10).

The above findings led us to examine whether CtIP is acetylated. A validated pan–acetyl-lysine (AcK) antibody (fig. S11A) detected CtIP (Fig. 4A) that had been purified from human cells (fig.

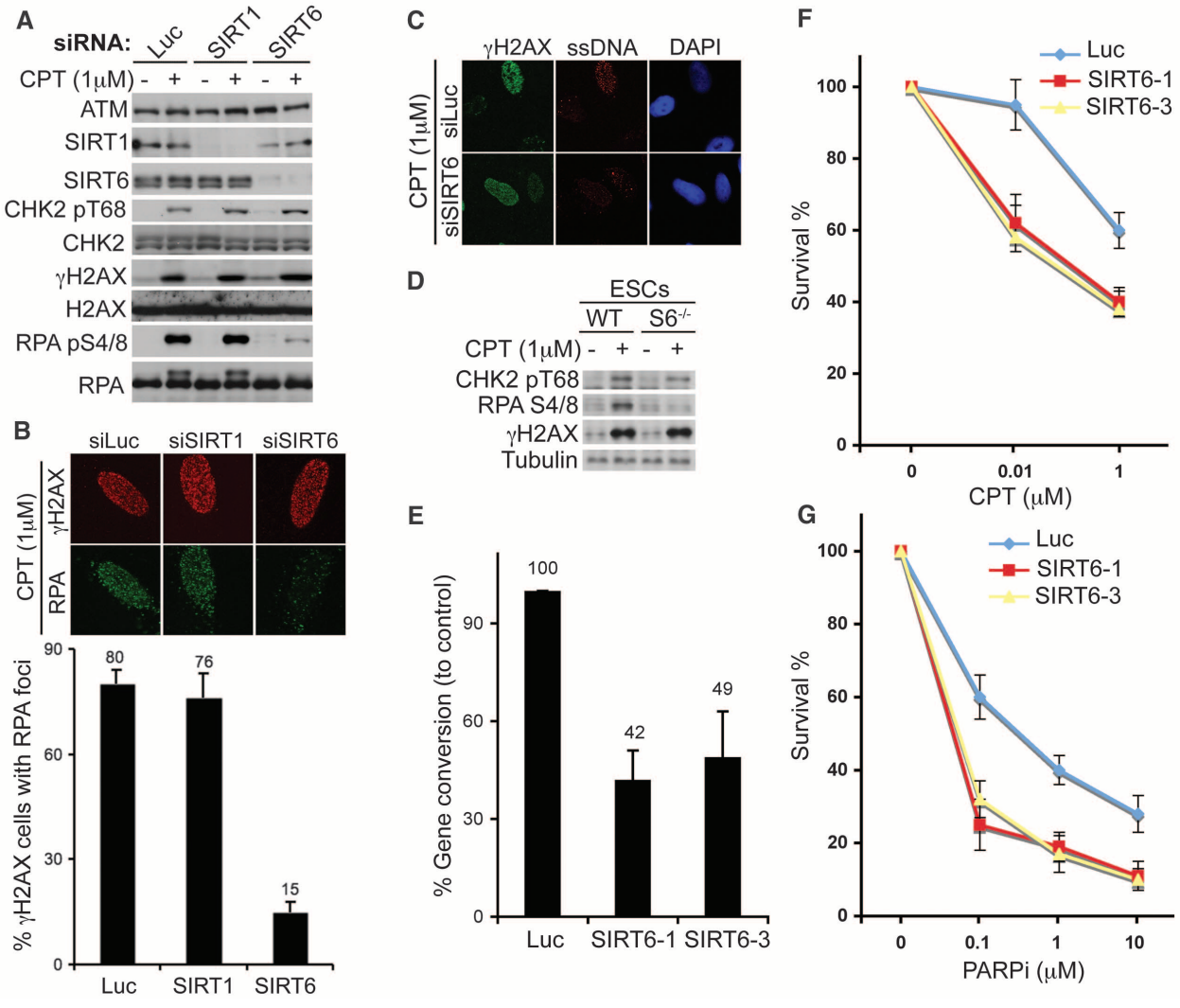

Fig. 2. SIRT6 promotes resection and homologous recombination. (**A**) SIRT1- and SIRT6- depleted U2OS cells were treated and analyzed. Luciferase siRNA (Luc) was used as control. (**B**) Upper panel: RPA immunofluorescence staining in U2OS cells after SIRT1 and SIRT6 depletion. Lower panel: Proportion of γH2AX-positive cells with RPA foci; 1000 cells were counted. (**C**) Immunofluorescence staining for ssDNA after SIRT6 depletion. (**D**) Mouse ESCs from wild-type (WT) or *Sirt6* knockout (S6$^{-/-}$) mice were treated and analyzed. (**E** to **G**) SIRT6 depletion impairs homologous recombination (E) and increases sensitivity to CPT (F) and PARP inhibitor (PARPi) (G). Data in (E) to (G) represent averages from three experiments ± SD.

S11C). Moreover, detection by this antibody was abrogated when CtIP was treated with purified wild-type SIRT6 (fig. S11B) in the presence of NAD^+ (Fig. 4A and fig. S11C). Thus, CtIP is acetylated in a manner that can be reversed by SIRT6. Next, we assessed whether CtIP acetylation was regulated in response to DNA damage. Although we readily detected acetylation of GFP-CtIP in undamaged cells, this acetylation was abrogated if cells were treated with CPT, etoposide, or ionizing radiation (Fig. 4B; note that we ruled out the possibility that CtIP phosphorylation after DNA damage prevents detection by the AcK antibody, fig. S12A). Furthermore, DNA damage–induced deacetylation of GFP-CtIP (Fig. 4C) or endogenous CtIP (Fig. 4D and fig. S12, B to D) was blocked when cells were treated with nicotinamide or wortmannin, which inhibits the apical DNA damage response protein kinases ATM (ataxia telangiectasia mutated), ATR (ATM and Rad3 related), and DNA-PK (DNA-dependent protein kinase). [In Fig. 4D, the apparent decrease of CtIP acetylation upon DNA damage in the presence of nicotinamide reflects phosphorylation affecting CtIP mobility (*5*), as confirmed in fig. S12C.] Although SIRT6 depletion prevented CtIP deacetylation after DNA damage (Fig. 4E), this CtIP deacetylation defect was complemented by wild-type SIRT6 but not by catalytically inactive SIRT6 (Fig. 4E). Thus, CtIP is constitutively acetylated and, after DNA damage, is deacetylated by SIRT6 to promote resection. However, nicotinamide treatment did not prevent CtIP recruitment kinetics to DNA damage sites (fig. S13) or DNA damage–induced CtIP phosphorylation (Fig. 4, D and E), which suggests that deacetylation promotes the ability of CtIP to mediate resection.

When we used a recently described CtIP DNA binding mutant (*6*) where Lys^{513} and Lys^{515} were mutated to Ala (2KA), this was not detected by the AcK antibody (Fig. 4F). However, mutating these residues to nonacetylatable arginines (2KR) restored CtIP detection by the AcK antibody (Fig. 4F). This indicated that, although these positions are not sites of CtIP acetylation, the positive charge of residues 513 and 515 is required for CtIP acetylation, possibly reflecting a prerequisite for DNA binding before CtIP can access, or be recognized by, its acetyltransferase. By purifying CtIP and subjecting it to mass spectrometry, we identified several CtIP acetylation sites, of which peptides containing Lys^{432}, Lys^{526}, and Lys^{604} had highest intensity (Fig. 4G and fig. S14). Mutating these three sites to alanine (CtIP-3KA) or arginine (CtIP-3KR) markedly reduced CtIP detection by the AcK antibody (Fig. 4F). Because CtIP-3KR was effectively recruited to DNA damage sites (fig. S15A) and complemented the phenotypes caused by CtIP depletion (fig. S15A), we tested whether CtIP-3KR expression might circumvent the requirement of SIRT6 for resection. Indeed, expression of CtIP-3KR, but not of wild-type CtIP, rescued RPA phosphorylation (Fig. 4H) and formation of RPA foci in cells depleted of endogenous CtIP and SIRT6 (Fig. 4I), and also partially alleviated the homologous recombination defect of such cells (Fig. 4J). Similarly, expression of CtIP-3KR relieved the inhibitory effect of nicotinamide on RPA phosphorylation (fig. S16). These findings establish CtIP as a key SIRT6 substrate by which SIRT6 promotes resection and DSB repair by homologous recombination.

Our findings support a model in which DNA damage triggers SIRT6-dependent CtIP deacetylation, thereby promoting resection and homologous

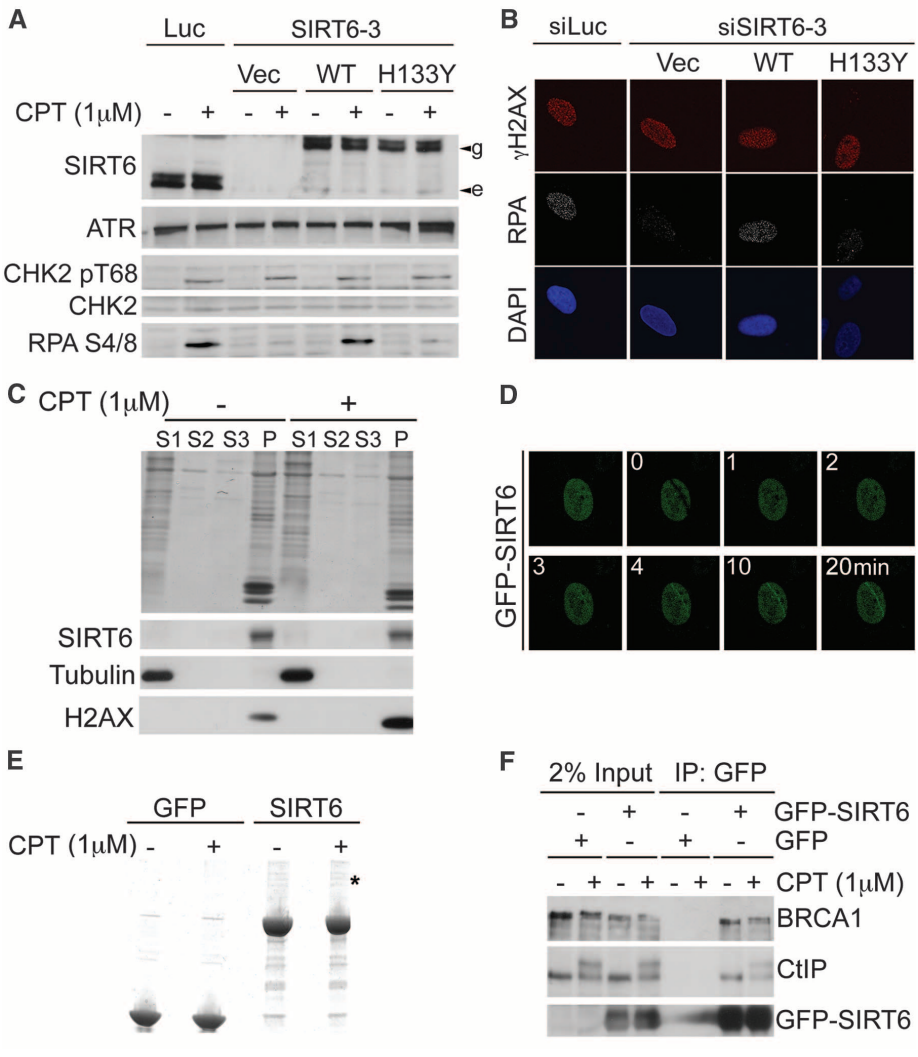

Fig. 3. SIRT6 recruitment to DNA damage sites and interaction with CtIP. (**A**) SIRT6 was depleted in U2OS cells stably expressing siRNA-resistant GFP-SIRT6 (WT or enzymatically inactive H133Y; e and g indicate endogenous and GFP-tagged SIRT6, respectively). (**B**) U2OS cells treated as in (A) were analyzed by immunofluorescence. (**C**) Fractionation of U2OS cells after CPT treatment: S1, cytoplasmic; S2, nuclear soluble; S3, 200 mM NaCl–extracted chromatin; P, pellet. (**D**) Recruitment kinetics of GFP-SIRT6 to laser-induced lesions. (**E**) Purified GFP-SIRT6 (asterisk denotes the band identified as CtIP). (**F**) Interaction between SIRT6 and CtIP by coimmunoprecipitation from U2OS cells stably transfected with GFP-SIRT6.

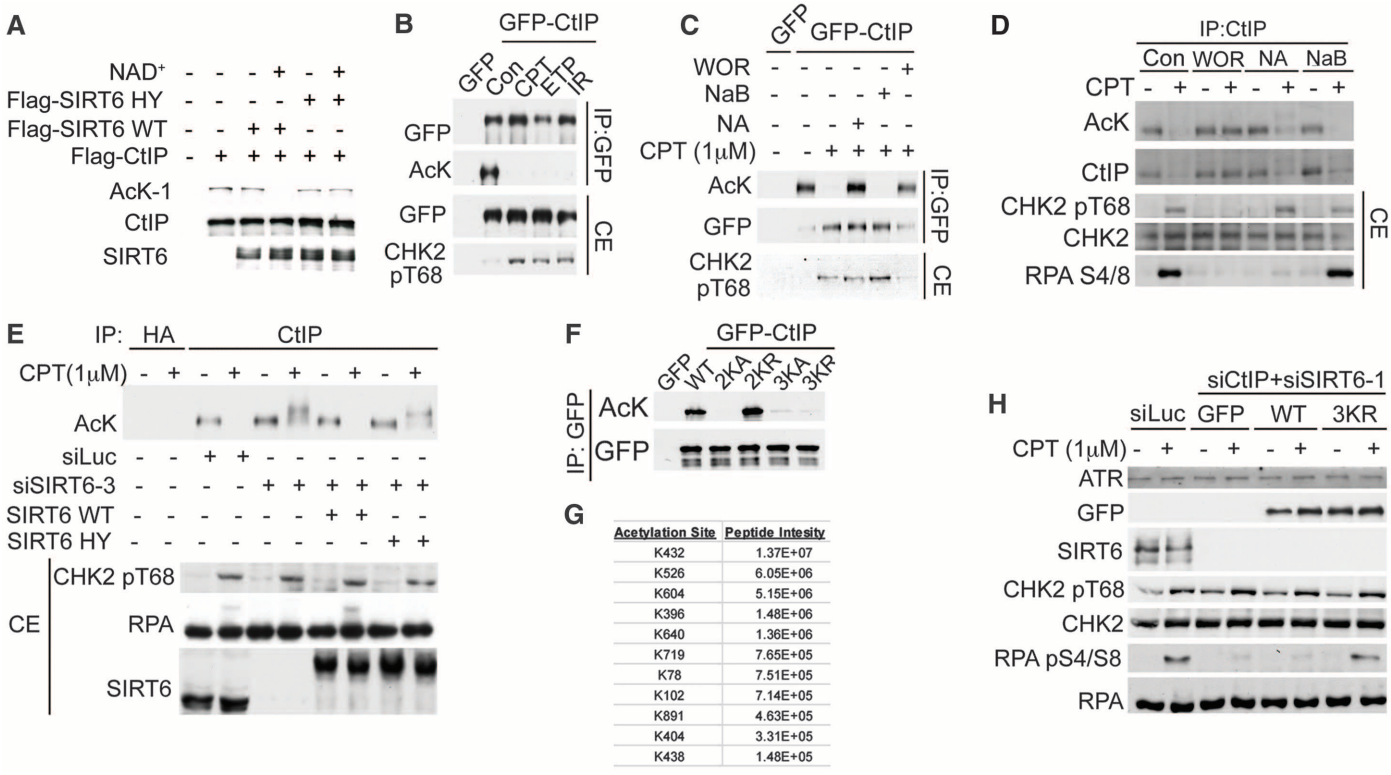

Fig. 4. SIRT6 deacetylates CtIP to promote resection and homologous recombination. (**A**) Constitutive CtIP acetylation is removed by SIRT6 in vitro after Flag-based purification from HEK293 cells. HY denotes the H133Y inactive mutant. (**B**) GFP-CtIP is acetylated in human embryonic kidney (HEK) 293 cells and deacetylated upon treatment with CPT (1 μM), etoposide (1 μM), or ionizing radiation (IR; 10 Gy). Immunoprecipitated material and cell extract (CE) were analyzed. (**C**) Nicotinamide or wortmannin (WOR) block GFP-CtIP deacetylation in HEK 293 cells after DNA damage. (**D**) Endogenous CtIP is acetylated in U2OS cells. A negative-control immunoprecipitation is shown in fig. S12D. (**E**) SIRT6 mediates CtIP deacetylation upon DNA damage. CtIP acetylation status is shown in U2OS cells stably expressing siRNA-resistant GFP-SIRT6. (**F**) Identification of CtIP acetylation sites. Mutations were introduced into GFP-CtIP and analyzed by immunoprecipitation and Western blotting. Mutants were 2KA (Lys^{513} and Lys^{515} → Ala), 2KR (Lys^{513} and Lys^{515} → Arg), 3KA (Lys^{432}, Lys^{526}, and Lys^{604} → Ala), and 3KR (Lys^{432}, Lys^{526}, and Lys^{604} → Arg). (**G**) Mass spectrometry data for intensity of acetylated CtIP peptides. (**H**) Nonacetylatable CtIP (3KR) alleviates resection defects caused by SIRT6 depletion. U2OS cells expressing siRNA-resistant GFP-CtIP (either wild-type or 3KR mutant), where SIRT6 and CtIP were depleted, were treated with CPT and analyzed. (**I**) U2OS cells treated as in (H) were analyzed by immunofluorescence. (**J**) CtIP-3KR mutant partially rescues homologous recombination defect of SIRT6-depleted cells. Cells contained vector (Vec), Flag-CtIP-WT, or 3KR. Data are from two experiments.

recombination. These results thereby establish that SIRT6 targets proteins in addition to histones (*17*, *23*), add to the known functions of SIRT6 in DNA base excision repair (*18*) and DSB repair by nonhomologous end joining (*21*), and help to explain the genome instability and premature aging phenotypes associated with SIRT6 loss in mice (*18*). Previous work has demonstrated cell cycle regulation of resection mediated via cyclin-dependent kinases regulating CtIP phosphorylation (*11*). We propose that CtIP deacetylation represents a further layer of control, presumably to ensure that resection only ensues at suitable times and locations.

References and Notes

1. C. Wyman, R. Kanaar, *Annu. Rev. Genet.* **40**, 363 (2006).
2. P. Sung, H. Klein, *Nat. Rev. Mol. Cell Biol.* **7**, 739 (2006).
3. P. Huertas, *Nat. Struct. Mol. Biol.* **17**, 11 (2010).
4. E. P. Mimitou, L. S. Symington, *DNA Repair* **8**, 983 (2009).
5. A. A. Sartori *et al.*, *Nature* **450**, 509 (2007).
6. Z. You *et al.*, *Mol. Cell* **36**, 954 (2009).
7. L. Chen, C. J. Nievera, A. Y.-L. Lee, X. Wu, *J. Biol. Chem.* **283**, 7713 (2008).
8. S. P. Jackson, J. Bartek, *Nature* **461**, 1071 (2009).
9. S. Lavu, O. Boss, P. J. Elliott, P. D. Lambert, *Nat. Rev. Drug Discov.* **7**, 841 (2008).
10. X. J. Yang, E. Seto, *Nat. Rev. Mol. Cell Biol.* **9**, 206 (2008).
11. P. Huertas, S. P. Jackson, *J. Biol. Chem.* **284**, 9558 (2009).
12. A. J. Pierce, P. Hu, M. Han, N. Ellis, M. Jasin, *Genes Dev.* **15**, 3237 (2001).
13. E. Michishita, J. Y. Park, J. M. Burneskis, J. C. Barrett, I. Horikawa, *Mol. Biol. Cell* **16**, 4623 (2005).
14. P. Oberdoerffer *et al.*, *Cell* **135**, 907 (2008).
15. R. H. Wang *et al.*, *Cancer Cell* **14**, 312 (2008).
16. D. B. Lombard, B. Schwer, F. W. Alt, R. Mostoslavsky, *J. Intern. Med.* **263**, 128 (2008).
17. E. Michishita *et al.*, *Nature* **452**, 492 (2008).
18. R. Mostoslavsky *et al.*, *Cell* **124**, 315 (2006).
19. H. E. Bryant *et al.*, *Nature* **434**, 913 (2005).
20. H. Farmer *et al.*, *Nature* **434**, 917 (2005).
21. R. A. McCord *et al.*, *Aging* **1**, 109 (2009).
22. X. Yu, L. C. Wu, A. M. Bowcock, A. Aronheim, R. Baer, *J. Biol. Chem.* **273**, 25388 (1998).
23. T. L. Kawahara *et al.*, *Cell* **136**, 62 (2009).

24. We thank all members of the Jackson laboratory for help and support; K. Miller and B. Xhemalce for advice on in vitro HDAC assays; J. Forment for help with analysis of PARP cleavage; K. Miller, R. Chapman, T. Oelschlaegel,

and K. Dry for advice on the manuscript; F. Alt for *Sirt6*$^{-/-}$ ESCs; R. Baer for CtIP antibodies; Y. Shiloh for ATM antibody; and S. West for RAD51 antibody. Research in the Jackson laboratory is supported by the European Community and a core infrastructure provided by Cancer Research UK and the Wellcome Trust. A.K. is funded by a Herchel Smith Fellowship. The Center for Protein Research is funded by a generous grant from the Novo Nordisk Foundation.

Supporting Online Material

www.sciencemag.org/cgi/content/full/329/5997/1348/DC1
Materials and Methods
Figs. S1 to S16
Tables S1 and S2

10 May 2010; accepted 22 July 2010
10.1126/science.1192049

Hemocyte Differentiation Mediates Innate Immune Memory in *Anopheles gambiae* Mosquitoes

Janneth Rodrigues, Fábio André Brayner,* Luiz Carlos Alves,* Rajnikant Dixit,† Carolina Barillas-Mury‡

Mosquito midgut invasion by ookinetes of the malaria parasite *Plasmodium* disrupts the barriers that normally prevent the gut microbiota from coming in direct contact with epithelial cells. This triggers a long-lived response characterized by increased abundance of granulocytes, a subpopulation of hemocytes that circulates in the insect's hemocoel, and enhanced immunity to bacteria that indirectly reduces survival of *Plasmodium* parasites upon reinfection. In mosquitoes, differentiation of hemocytes was necessary and sufficient to confer innate immune memory.

The innate immune system is thought to be hard-wired and unable to establish immunological memory (*1*). Insects lack adaptive immunity and rely on the innate immune system to mount defense responses against pathogenic organisms; however, memory-like responses have been described in invertebrates, a phenomena that has been termed immune priming (*2*). There are multiple examples of nonspecific (*3*–*5*) and pathogen-specific (*6*–*11*) priming in insects that can be long-lasting. Although these studies challenge the dogma that invertebrates are incapable of adaptive immune responses, a mechanism for innate immune memory has not been established.

Anopheles gambiae mosquitoes are the major vectors of *Plasmodium falciparum* malaria in Africa. In the present study, we found that *Plasmodium* ookinete invasion of the mosquito midgut in the presence of gut bacteria primed a robust long-lived enhanced antibacterial response that also reduced *Plasmodium* survival upon rechallenge. Immune priming resulted in quantitative and qualitative differentiation of hemocytes, the insect equivalent of white blood cells, that persisted for the lifespan of the mosquito.

We investigated the effect of preexposure of mosquitoes to *Plasmodium* infection on a subsequent infection (fig. S1) (*12*). Two groups of mosquitoes were fed on the same infected mouse. One group was placed at 28°C immediately after blood feeding, a temperature that prevents *Plasmodium berghei* ookinete formation and mosquito infection (fig. S2). We refer to these mosquitoes as the naïve group. The challenged group was kept at 21°C for 48 hours to allow ookinete formation and midgut invasion and was then switched to 28°C to reduce oocyst survival (fig. S2). Seven days postfeeding (dpf), both groups were infected by feeding on a second mouse. Reexposure to *Plasmodium* infection greatly reduced the intensity of infection in the challenged group (Fig. 1A) ($P < 0.005$). This immune enhancement was also observed in females rechallenged 14 days postpriming (dpp) ($P < 0.0005$) (Fig. 1B). The time between priming and rechallenge was not extended because of age-related mosquito mortality. Preexposure of mosquito females to *P. falciparum* (NF54 strain) infection had a similar effect, reducing oocyst density when rechallenged with the same parasite ($P < 0.05$, Mann-Whitney test) (Fig. 1C and fig. S3).

Large numbers of commensal bacteria are present in the midgut lumen when *Plasmodium* ookinetes invade epithelial cells. The blood meal is surrounded by a chitinous peritrophic matrix (PM) that normally prevents bacteria from interacting directly with epithelial cells, but ookinetes disrupt this barrier (*13*) to invade midgut cells (fig. S4), causing irreversible damage (*14*). The PM sac containing the blood-meal remnants is expelled when digestion is completed, and a new PM sac forms with each subsequent feeding. Elimination of the gut microbiota enhances *Plasmodium* infection (*15*–*17*), and activation of some mosquito antibacterial responses have been shown to indirectly kill *Plasmodium* (*17*).

Gut bacteria were eliminated by oral administration of antibiotics before the first feeding (fig. S1, yellow area), which prevented immune priming to *Plasmodium* (Fig. 1D). Then priming was allowed to occur in the presence of bacteria, but antibiotics were given 2 days before the second infection (fig. S1, beige area). Elimination of the gut microbiota when mosquitoes are rechallenged prevented elicitation of the priming response (Fig. 1E). It was the interaction between bacteria and invaded midgut cells that appeared to elicit the response, which indicates that the decrease in *Plasmodium* infection in the challenged group (Fig. 1, A and B) was not due to persistent immune activation in response to the first plasmodial infection.

The effect of priming on mosquito commensal bacteria was investigated. Total bacteria in challenged mosquitoes 7 dpp were 1% of the amount in naïve mosquitos ($P < 0.005$) (Fig. 2A). Bacterial levels in the midgut were similar between

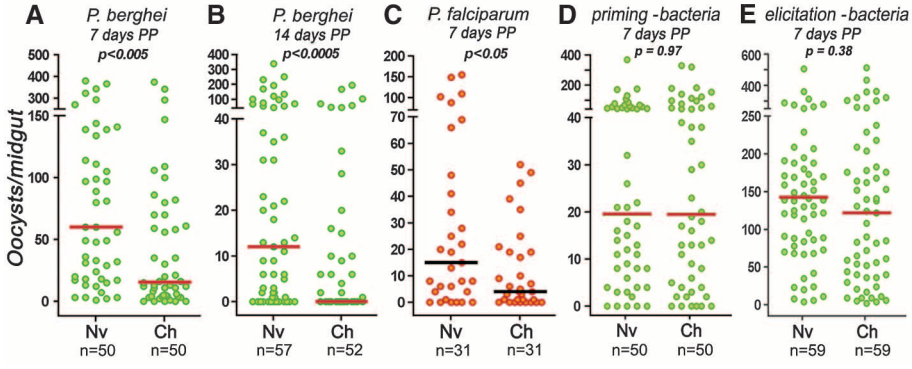

Fig. 1. Effect of preexposure to *Plasmodium* infection on the immune response to subsequent infections. (**A**) 7 dpp and (**B**) 14 dpp with *P. berghei* in naïve (Nv) or challenged (Ch) mosquitoes. (**C**) Effect of prechallenge with *P. falciparum* on a second infection at 7 dpp. *Plasmodium* infections were evaluated 7 days after the second infection. Effect of eliminating the gut microbiota with oral antibiotics before the (**D**) first and (**E**) second challenge with *P. berghei* on a second infection 7 dpp. Each circle represents the number of parasites in an individual midgut, and lines indicate the medians.

Laboratory of Malaria and Vector Research, National Institute of Allergy and Infectious Diseases, National Institutes of Health, Rockville, MD 20892, USA.

*Present address: Centro de Pesquisas Aggeu Magalhães (CPqAM/Fiocruz) and Laboratório de Imunopatologia Keizo Asami–Universidade Federal de Pernambuco, Pernambuco, Recife, Brazil.

†Present address: National Institute of Malaria Research, Sector-8, Dwarka, New Delhi-110077, India.

‡To whom correspondence should be addressed. E-mail: cbarillas@niaid.nih.gov